

Percolation in real interdependent networks

Filippo Radicchi¹

¹*Center for Complex Networks and Systems Research,
School of Informatics and Computing, Indiana University, Bloomington, USA**

The function of a real network depends not only on the reliability of its own components, but is affected also by the simultaneous operation of other real networks coupled with it. Robustness of systems composed of interdependent network layers has been extensively studied in recent years. However, the theoretical frameworks developed so far apply only to special models in the limit of infinite sizes. These methods are therefore of little help in practical contexts, given that real interconnected networks have finite size and their structures are generally not compatible with those of graph toy models. Here, we introduce a theoretical method that takes as inputs the adjacency matrices of the layers to draw the entire phase diagram for the interconnected network, without the need of actually simulating any percolation process. We demonstrate that percolation transitions in arbitrary interdependent networks can be understood by decomposing these system into uncoupled graphs: the intersection among the layers, and the remainders of the layers. When the intersection dominates the remainders, an interconnected network undergoes a continuous percolation transition. Conversely, if the intersection is dominated by the contribution of the remainders, the transition becomes abrupt even in systems of finite size. We provide examples of real systems that have developed interdependent networks sharing a core of “high quality” edges to prevent catastrophic failures.

Percolation is among the most studied topics in statistical physics [1]. The model used to mimic percolation processes assumes the existence of an underlying network of arbitrary structure. Regular grids are traditionally considered to model percolation in materials [2, 3]. Complex graphs are instead assumed as underlying supports in the analysis of spreading phenomena in social environments [4, 5], or in robustness studies of technological and infrastructural systems [6–8]. Once the network has been specified, a configuration of the percolation model is generated assuming nodes (or sites) present with probability p . For $p = 0$, only a disconnected configuration is possible. For $p = 1$ instead, all nodes are within the same connected cluster. As the occupation probability varies, the network undergoes a structural transition between these two extreme configurations. Although there are special substrates, e.g., one-dimensional lattices, where the percolation transition may be discontinuous, in the majority of the cases, random percolation models give rise to continuous structural changes [9]. This means that the size of the largest cluster in the network, used as a proxy for the connectedness of the system, increases from the non-percolating to the percolating phases in a smooth fashion.

The percolation transition may become discontinuous in a slightly different model involving not just a single network, but a system composed of two or more interdependent graphs [10]. This is a very realistic scenario considering that many, if not all, real graphs are “coupled” with other real networks. Examples can be found in several domains: social networks (e.g., Facebook, Twitter, etc.) are coupled because they share the same actors [11];

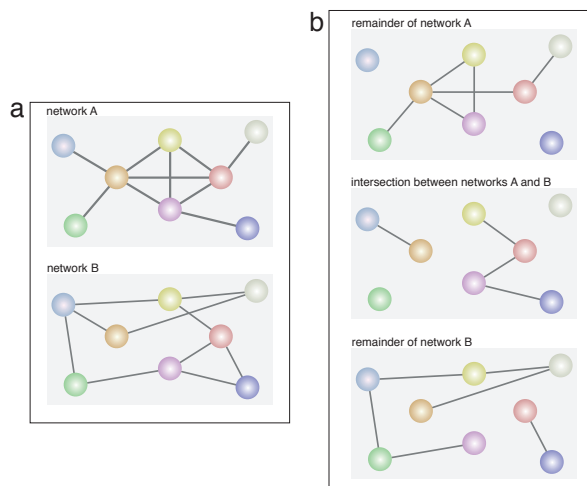


Figure 1: Decomposition of interconnected networks into uncoupled graphs. **a)** Schematic example of two coupled networks A and B . In this representation, nodes of the same color are one-to-one interdependent. **b)** In the percolation model, the interconnected system is equivalent to a set of three graphs that do not share any edge: the remainders of the network layers A and B , and their intersection.

multimodal transportation networks are composed of different layers (e.g., bus, subway, etc.) that share the same locations [12, 13]; the functioning of communication and power grid systems depend one on the other [10]. In the simplest case, one considers an interconnected system composed of only two network layers. Nodes in both layers are uniquely identified, but the way they are connected to the other vertices is not necessarily identical (see Fig. 1). In the percolation model defined on this system, nodes are still present with probability p . Since

*Electronic address: filiradi@indiana.edu.

the networks are interdependent, the presence of a node in one layer implies the presence of the same vertex in the other layer. However, as p varies, one node may not be simultaneously within the largest clusters of both layers. In such a case, the vertex is said to be outside the largest cluster of mutually connected nodes. This is a set of nodes identified in a recursive manner, and composed of vertices that are simultaneously in the largest clusters of both network layers thanks only to connections with other nodes within the set. It has been proved that, in infinitely large interconnected systems composed of two uncorrelated random networks, the percolation transition, monitored through the size of the largest cluster of mutually connected nodes, is discontinuous [10, 14, 15]. This result has been however shown to not apply to more general network models that account for degree correlations [16, 17]. Unfortunately, all these theoretical approaches have been developed under two special, and unrealistic, assumptions. First, they hypothesize that network layers are generated according to some kind of graph toy model whose topology is not specified by a one-zero adjacency matrix, but rather a list of probabilities for pairs of nodes to be connected. Second, they apply only to the case of infinitely large systems. Real interdependent networks, on the other hand, are composed of layers very different from those that can be generated with toy models, and they clearly have finite size. In this paper, we introduce a novel theoretical approach of direct applicability to the study of percolation transitions in real interdependent networks.

To illustrate our methodology, we start from a simplified version of a recent theory developed for percolation in real isolated networks [18–20]. Consider an undirected and unweighted graph composed of N nodes and E edges. The structure of the graph is encoded by the adjacency matrix A , a symmetric $N \times N$ matrix whose generic element A_{ij} differs from zero and equals one only if vertices i and j share an edge. Without loss of generality, we assume that, when all nodes are present in the network, the graph is formed by a single connected component. Let us consider an arbitrary value of the site occupation probability $p \in (0, 1)$, and indicate with s_i the probability that the generic node i is part of the largest cluster. The order parameter of the percolation transition is simply defined as the average of these probabilities over all nodes in the graph, i.e., $P_\infty = \frac{1}{N} \sum_i s_i$. Note that s_i is a function of p , but, in the following, we omit this dependence for shortness of notation. As a first attempt, we can say that the probability s_i for node i to be part of the largest cluster is given by

$$s_i = p \left[1 - \prod_{j \in \mathcal{N}_i} (1 - s_j) \right], \quad (1)$$

where \mathcal{N}_i is the set of neighbors of vertex i . The probability s_i is written as the product of two contributions: (i) the probability that the node is occupied; (ii) the probability that at least one of its neighbors is part of the largest cluster. The attempt of Eq. (2) relies on the so-

called locally tree-like approximation [9]. In this ansatz, neighbors of node i are not directly connected, and this allows us to consider the probabilities s_j as independent variables. This approximation typically holds in real networks [19], but does not apply to regular lattices. Introducing the vectors \vec{u} and \vec{q} , whose i -th components are respectively $u_i = \ln(1 - s_i)$ and $q_i = \ln(1 - s_i/p)$, we can write the set of coupled equations (1) into the single vectorial equation

$$\vec{q} = A \vec{u} \quad (2)$$

A trivial solution of Eq. (2) is given by the configuration $\vec{u} = \vec{q} = \vec{0}$, corresponding to $\vec{s} = \vec{0}$ or $s_i = 0$ for all $i = 1, \dots, N$. In the proximity of this configuration, we can make use of the truncated Taylor expansion $\ln(1 - x) = -x$, and Eq. (2) reads as

$$\vec{s} = p A \vec{s}, \quad (3)$$

thus an eigenvalue/eigenvector equation. By the Perron-Frobenius theorem, the only solution having a physical meaning of this equation is obtained by setting $p = 1/\lambda$ and $\vec{s} = \vec{l}$, with (λ, \vec{l}) principal eigenpair of the adjacency matrix A . This tells us that the solution of Eq. (1) is $s_i = 0$, for all $i = 1, \dots, N$, if the site occupation probability is smaller than $1/\lambda$. In this region, the network is in the non-percolating regime. Slightly on the right of $1/\lambda$, the vector of probabilities \vec{s} starts to grow in the direction of the principal eigenvector of the adjacency matrix, and the order parameter is not longer zero. For any value of the site occupation probability larger than $1/\lambda$, the network is in the percolating phase. The site percolation threshold obtained using the approximation of Eq. (1) is thus $p_c = 1/\lambda$. Further, Eq. (1) can be solved numerically to draw the percolation diagram of the network in this approximation.

The most serious limitation of Eq. (1) is to introduce a positive feedback among probabilities. An increment in the probability s_i produces an increase in the probabilities s_j of the neighbors, which in turn causes an increment in the probability s_i , and so on. To avoid the presence of this self-reinforcement effect, we can rewrite Eq. (1) as

$$s_i = p \left[1 - \prod_{j \in \mathcal{N}_i} (1 - r_{i \rightarrow j}) \right]. \quad (4)$$

This equation still relies on the locally tree-like ansatz. Here, $r_{i \rightarrow j}$ stands for the probability that node j is part of the largest cluster independently of vertex i . We note that, while this quantity can be defined for any pair of nodes, only contributions given by adjacent vertices play a role in Eq. (4). We can think $r_{i \rightarrow j}$ as one of the $2E$ components of a vector \vec{r} . In the definition of \vec{r} , every edge (i, j) in the graph is responsible for two entries, i.e., $r_{i \rightarrow j}$ and $r_{j \rightarrow i}$. For consistency, the probability $r_{i \rightarrow j}$ obeys

$$r_{i \rightarrow j} = p \left[1 - \prod_{k \in \mathcal{N}_j \setminus \{i\}} (1 - r_{j \rightarrow k}) \right]. \quad (5)$$

The product of the r.h.s. of the last equation runs over all neighbors of node j excluding vertex i . It is convenient to rewrite Eq. (5) as $\ln(1 - r_{i \rightarrow j}/p) = \sum_k A_{jk} \ln(1 - r_{j \rightarrow k}) - A_{ji} \ln(1 - r_{j \rightarrow i})$. Defining the vectors \vec{w} and \vec{t} such that their $(i \rightarrow j)$ -th components are respectively given by $w_{i \rightarrow j} = \ln(1 - r_{i \rightarrow j})$ and $z_{i \rightarrow j} = \ln(1 - r_{i \rightarrow j}/p)$, the system of equations (5) becomes equivalent to the vectorial equation

$$\vec{t} = M \vec{w}. \quad (6)$$

The generic element of the $2E \times 2E$ square matrix M is given by

$$M_{i \rightarrow j, k \rightarrow \ell} = \delta_{j,k} (1 - \delta_{i,\ell}), \quad (7)$$

where $\delta_{x,y}$ is the Kronecker delta function defined as $\delta_{x,y} = 1$ if $x = y$, and $\delta_{x,y} = 0$, otherwise. Thus, the generic entry of the matrix M is different from zero only if the ending node of the edge $i \rightarrow j$ corresponds to the starting vertex of the edge $k \rightarrow \ell$, but the starting and ending nodes i and ℓ are different. This matrix is known as the non-backtracking matrix of the graph [21, 22]. A trivial solution of the preceding equation is given by $\vec{r} = \vec{0}$, which in turn leads to $\vec{s} = \vec{0}$. In proximity of this configuration, we can still make use of the truncated Taylor expansion of the logarithm, and rewrite Eqs. (4) and (6) respectively as

$$s_i = p \sum_j A_{ij} r_{i \rightarrow j} \quad \text{and} \quad \vec{r} = p M \vec{r}. \quad (8)$$

Using arguments similar to those applied to Eq. (3), we can say that, according to Eq. (8), the percolation threshold equals $p_c = 1/\mu$, with μ principal eigenvalue of the non-backtracking matrix of the graph, and that slightly on the right of the critical point the probability s_i grows linearly with the sum of the components of the principal eigenvector of the non-backtracking matrix corresponding to edges pointing out from node i . The entire percolation diagram can be instead obtained by numerically solving the system of Eqs. (4) and (5).

To summarize, the results presented so far tell us two main interesting things. First, the difference between the two approaches resides only in the inclusion or exclusion of self-reinforcement effects among local variables. In this sense, Eqs. (4) and (5) represent an improvement to Eq. (1), but both approaches are based on the same principles and approximations. This first observation serves to reunite recent predictions on percolation thresholds under the same theory [18–20]. Second, the way in which individual probabilities behave slightly on the right of the critical point allow us to understand why the prediction of the percolation threshold of Eq. (8) may become inaccurate in networks with localized eigenstates of the non-backtracking matrix [23].

Next, we propose the generalization of the previous equations to describe percolation transitions in two interdependent networks. Indicate with A and B the adjacency matrices of the two network layers. Our first

attempt to write the the probability s_i that node i is in the largest mutually connected cluster of the system is given by

$$s_i = p [S_{\mathcal{AB}_i} + (1 - S_{\mathcal{AB}_i}) S_{\mathcal{A}-\mathcal{B}_i} S_{\mathcal{B}-\mathcal{A}_i}], \quad (9)$$

where $S_{\mathcal{X}} = 1 - \prod_{j \in \mathcal{X}} (1 - s_j)$ is the probability that at least one of the nodes j in the set \mathcal{X} is part of the largest cluster (for the empty set \emptyset , we have $S_{\emptyset} = 0$). In the definition of Eq. (9), we have implicitly defined three disjoint sets of nodes: $\mathcal{AB}_i = \mathcal{N}_i^A \cap \mathcal{N}_i^B$ is the set of nodes that are neighbors of vertex i in both layers, $\mathcal{A} - \mathcal{B}_i = \mathcal{N}_i^A \setminus \mathcal{AB}_i$ is the set of nodes connected to vertex i only in layer A but not in B , and $\mathcal{B} - \mathcal{A}_i = \mathcal{N}_i^B \setminus \mathcal{AB}_i$ is the set of nodes that are neighbors of vertex i in layer B but not in A . Eq. (9) essentially states that, given that the vertex is occupied, the probability s_i for node i of being part of the largest mutually connected cluster is given by the sum of two contributions: (i) the probability to be connected to the largest cluster thanks to at least one vertex that is connected to i in both layers; (ii) if the latter condition is not true, the probability that node i is connected to the largest cluster through at least one node k in layer A and one node ℓ in layer B , with $k \neq \ell$. Note that, if the network layers are identical, then Eq. (9) correctly reduces to Eq. (1). In other terms, one can split the set of edges in the system in three different subset, and then construct three different graphs on the basis of this unique division (see Fig. 1): the intersection graph with adjacency matrix given by the Hadamard product of the matrices A and B [i.e., the (i, j) -th element of the adjacency matrix is $A_{ij} B_{ij}$]; the remnant of network A , where edges between nodes i and j are present only if $A_{ij}(1 - B_{ij}) = 1$; the remainder of graph B , whose (i, j) -th adjacency matrix element equals $B_{ij}(1 - A_{ij})$. If we make use of the vector \vec{u} previously defined, we can write $S_{\mathcal{AB}_i} = 1 - \exp[-\sum_j A_{ij} B_{ij} u_j]$, $S_{\mathcal{A}-\mathcal{B}_i} = 1 - \exp[-\sum_j A_{ij}(1 - B_{ij}) u_j]$ and $S_{\mathcal{B}-\mathcal{A}_i} = 1 - \exp[-\sum_j B_{ij}(1 - A_{ij}) u_j]$. Thus, the numerical solution of Eq. (9) can be obtained in a certain number of iterations, each having a computational complexity that grows at maximum as the number of edges present in the denser layer. Unfortunately, the Taylor expansion of the r.h.s. of Eq. (9) gives us only some insights about the structure of the solution, but it does not allow to reduce the original problem to a simple eigenvalue/eigenvector equation as in the case of isolated networks (see Appendix).

Also here, we can avoid the presence of self-reinforcing mechanisms among variables by excluding already visited edges. The equations read as

$$s_i = p [R_{\mathcal{AB}_i} + (1 - R_{\mathcal{AB}_i}) R_{\mathcal{A}-\mathcal{B}_i} R_{\mathcal{B}-\mathcal{A}_i}], \quad (10)$$

and

$$r_{i \rightarrow j} = p [R_{\mathcal{AB}_j \setminus \{i\}} + (1 - R_{\mathcal{AB}_j \setminus \{i\}}) R_{\mathcal{A}-\mathcal{B}_j \setminus \{i\}} R_{\mathcal{B}-\mathcal{A}_j \setminus \{i\}}], \quad (11)$$

with $R_{\mathcal{X}_i} = 1 - \prod_{j \in \mathcal{X}} (1 - r_{i \rightarrow j})$, and the three sets \mathcal{AB}_i , $\mathcal{A} - \mathcal{B}_i$ and $\mathcal{B} - \mathcal{A}_i$ are defined as above. If the

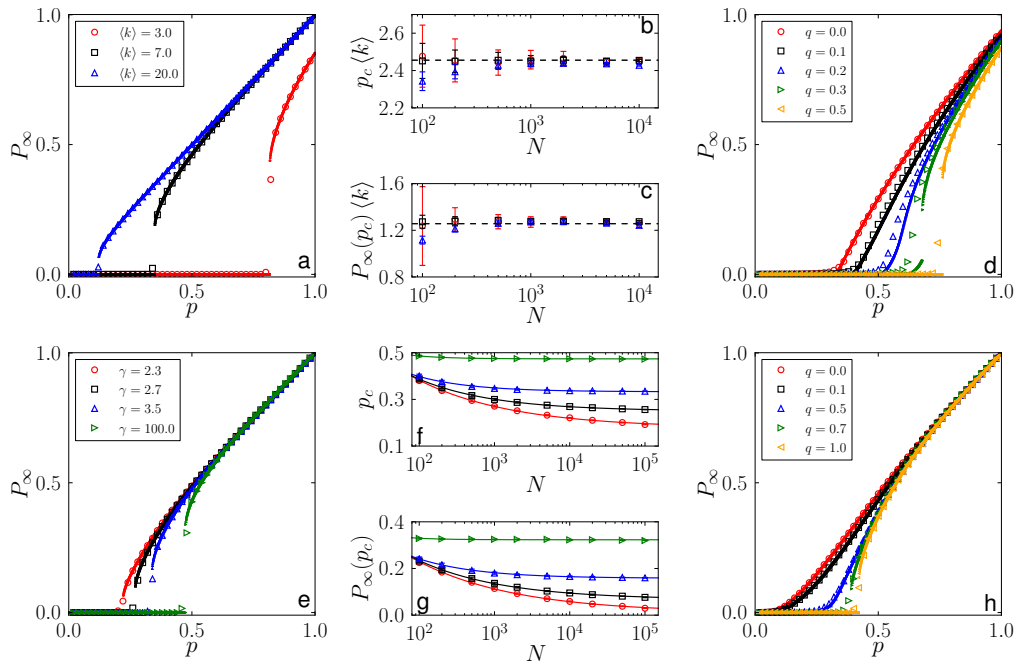


Figure 2: Percolation transition in artificial interconnected networks. **a)** Percolation diagrams for interdependent Erdős-Rényi graphs. We generate network layers with the same average degree $\langle k \rangle$, and compare results of numerical simulations (large symbols) with the solutions of our equations (small symbols). Results are obtained on a single instance of the network model, where both layers have size $N = 10^4$. Different colors and symbols refer to different values of the average degree $\langle k \rangle$. **b)** and **c)** For a given size of the network layers, we generate several instances of the model, and compute the percolation threshold p_c and the height of the order parameter at criticality $P_\infty(p_c)$. Both quantities are multiplied by the average degree $\langle k \rangle$. Points refer to average values obtained over several realizations of the graph model, while error bars stand for standard deviations. We use the same symbols and colors as those of panel a. Results are compared with the theoretical expected values $p_c(\langle k \rangle) = 2.4554$ and $P_\infty(p_c)\langle k \rangle = 1.2564$ (dashed black lines). **d)** We generate a single Erdős-Rényi graph with $N = 10^4$ and $\langle k \rangle = 3.0$, and use it as structure for both layers. We then exchange with probability q the label of every node of layer B with a randomly selected vertex. **e)** Percolation diagrams for single instances of interdependent scale-free networks. Each layer is obtained by randomly connecting vertices whose degrees obey the distribution $P(k) \sim k^{-\gamma}$, if $k \in [5, \sqrt{N}]$, and $P(k) = 0$, otherwise. Here, $N = 10^4$. **f)** and **g)** We compute the average values of p_c and $P_\infty(p_c)$ in several realizations of model composed of interdependent scale-free networks with size N . Standard deviations have size comparable with those of the symbol sizes. We use the same symbol/color scheme as in panel e. Full lines in panel f stand for best estimates of fits of empirical points with the function $p_c(N) = p_c + N^{-\alpha}$. The same type of functions are used in panel g to extrapolate the asymptotic value of $P_\infty(p_c)$. For any value of the degree exponent, we find that the asymptotic values of both quantities are strictly larger than zero (see Appendix). **h)** We generate a graph with $N = 10^4$ nodes, and degrees extracted from a power-law distribution with exponent $\gamma = 2.5$ and support $[3, \sqrt{N}]$. We use this network as structure for both layers. We then exchange with probability q the label of every node of layer B with a randomly selected vertex.

network layers are identical, then Eqs. (10) and (11) reduce to Eqs. (4) and (5). If we indicate with $\vec{r}^{(AB)}$ the vector whose components are generated by edges present in the intersection graph, $\vec{w}^{(AB)}$ the vector with entries of the type $w_{i \rightarrow j}^{(AB)} = \ln(1 - r_{i \rightarrow j}^{(AB)})$, and $M^{(AB)}$ the non-backtracking matrix obtained from the adjacency matrix of intersection between layers, we can write $R_{\mathcal{A}B_j \setminus \{i\}} = 1 - \exp[M^{(AB)} \vec{w}^{(AB)}]$. In a similar spirit, we can also write $R_{\mathcal{A} \setminus B_j \setminus \{i\}} = 1 - \exp[M^{(A-B)} \vec{w}^{(A-B)}]$ and $R_{B \setminus \mathcal{A}_j \setminus \{i\}} = 1 - \exp[M^{(B-A)} \vec{w}^{(B-A)}]$, where these equations are valid only for edges that belong to either layer A or layer B . Obtaining a numerical solution of Eqs. (10) and (11) by iteration is thus relatively fast,

since every iteration has a computational complexity at maximum equal to twice the number of edges present in the denser network layer. This is a great achievement given the high complexity of the algorithm necessary to draw the phase diagram for the percolation process in interdependent networks by means of direct numerical simulations [24].

Phase diagrams obtained through the numerical solution of Eqs. (10) and (11) reproduce the results of numerical simulations very accurately. In Fig. 2a for example, we consider systems composed of two independent Erdős-Rényi network models with different values of the average degree $\langle k \rangle$, where each network layer is generated by connecting pairs of vertices with probability $\langle k \rangle/N$. A fun-

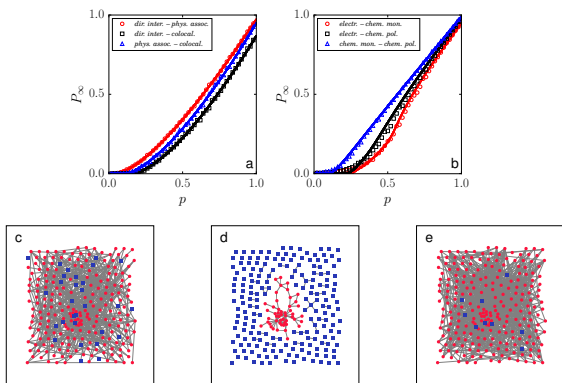


Figure 3: Percolation transition in interdependent biological networks. **a)** Phase diagram for the multilayer *H. sapiens* protein interaction network [25, 26]. Edges in different layers represent diverse type of connections among proteins: direct interaction, physical association, and colocalization. When analyzing a multiplex with two of these layers, we restrict our attention only on the set of nodes present in both layers. For each of the three systems formed by two interconnected networks that we can generate with this data, we draw the percolation diagram by means of numerical simulations (large symbols) and numerical solution of our equations (small symbols). **b)** Phase diagram for the multilayer network of the *C. elegans* connectome [26]. Edges in different layers represent different types of synaptic junctions among the neurons: electrical, chemical monadic, and chemical polyadic. **c)** Decomposition of the multilayer *C. elegans* connectome. Remnant of the layer corresponding to electrical junctions, **d)** intersection among the layers corresponding to electrical and chemical monadic interactions and **e)** remainder of the layer corresponding to chemical monadic junctions. In the various panels, nodes belonging to the largest connected component are visualized with red circles. All other nodes are instead represented with blue squares.

damental feature that the diagrams reveal is the presence of a sudden jump in the order parameter P_∞ at a certain threshold p_c . We stress that our equations predict the existence of first-order percolation transitions in networks of finite size, and not just in the thermodynamic limit. As Figs. 2b and c show, the location of the critical point p_c , and the height of the jump of the order parameter are well described by predictions valid for this type of graph models in the limit of infinite size [10, 14, 15]. We argue that a sudden jump in the order parameter is present only if the contribution of the remainders dominates the importance of the intersection. This condition is certainly verified in interdependent Erdős-Rényi graphs, where the intersection is composed of a very small number of edges, roughly equal to $\langle k \rangle / 2$, while the number of edges in each remnant is proportional to $\langle k \rangle N / 2$. Our intuition is fully supported by the results of Fig. 2d. Here, we control for the weight of the intersection with respect to those of the remainders in a simple fashion [28]. The two layers are given by exactly the same network structure.

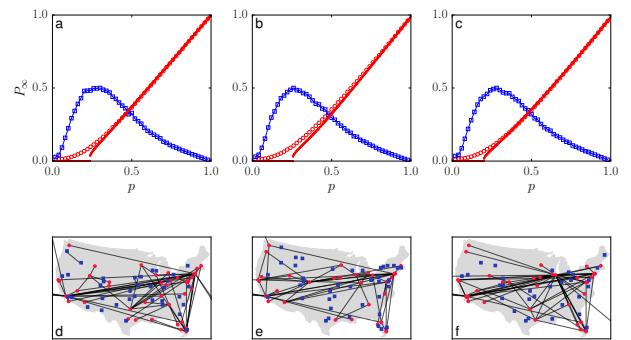


Figure 4: Percolation transition in interconnected transportation networks. **a)** The system is obtained by combining Delta and American Airlines routes. We consider only US domestic flights operated in January, 2014 [27], and construct an interconnected network where airports are nodes, and connections on the layers are determined by the existence of at least a flight between the two locations. In the percolation diagram, large red circles are results of numerical simulations, whereas small red circles represent the solutions of our equations. Blue squares represent susceptibility, a measure of the fluctuation across realizations of the percolation model, whose peak location is often used as a proxy for the identification of the critical threshold p_c . **b)** Same as in a, but for the combination of Delta and United flights. **c)** Same as in a, but for the combination of American Airlines and United flights. **d, e, and f)** Intersection graphs for the systems analyzed respectively in panels a, b and c. In the various network visualizations, nodes belonging to the largest connected component are visualized with red circles. All other nodes are instead represented with blue squares.

Indices of interdependent nodes are however shuffled with a given probability q . As q grows, the percolation transition changes its features: we pass from a continuous phase transition for small values of q , through a mix between a second- and a first-order structural change at intermediate values of q , to a discontinuous phase transition for sufficiently large values of q . The same type of considerations hold when network layers are scale-free random graphs. The transition is always discontinuous if the layers are uncorrelated, so that only remainders are present (Fig. 2e). This can be viewed by the existence of a finite value of the critical threshold p_c (Fig. 2f), and a jump of non null height of the order parameter at criticality (Fig. 2g). Still, the nature of the phase transition can be tuned from first to second order by simply decreasing the density of the intersection relatively to those of the remainders (Fig. 2h). Our argument about the dependence of the nature of the transition on the weight of the intersection compared to those of the remainders may serve to explain why real interdependent networks are not exposed to catastrophic failures [17]. In Fig. 3, we draw the percolation diagrams for two interconnected systems of interest in the biological sciences: the *H. sapiens* protein interaction network [25, 26], and the *C. elegans* connectome [26]. Both these interconnected sys-

tems undergo continuous percolation transitions. Interestingly, this behavior is not caused by the amount of redundancy among layers, but rather the “quality” of the edges shared across layers. Connections in the intersection graph account, in fact, for less than 10% in five out of the six interdependent networks analyzed here. It seems therefore that these organisms have developed interconnected networks sharing a core of “high quality” edges to prevent catastrophic failures. Whereas the robustness we observe in biological networks can be viewed as the result of a selective evolutionary process, one may argue that man-made interdependent systems could have been instead not perfectly designed to resist to random

damages of their components. This is indeed what arise from the analysis of the multilayer air transportation network within the US (Fig. 4) [29, 30]. The system shows fragility, with a sudden jump of the order parameter. On the other hand, the height of the jump is not as dramatic as observed in random uncorrelated graphs. Major airports all belong to the largest connected component of the intersection graph, and their connections constitute a set of high quality edges that avoid truly catastrophic changes in the connectedness of the entire interdependent system. From these examples, it seems therefore that real interdependent networks may be not so fragile as previously believed.

-
- [1] D. Stauffer and A. Aharony, *Introduction to percolation theory* (Taylor and Francis, 1991).
- [2] S. Kirkpatrick, *Reviews of modern physics* **45**, 574 (1973).
- [3] B. Berkowitz, *Mathematical Geology* **27**, 467 (1995).
- [4] R. Pastor-Satorras and A. Vespignani, *Physical review letters* **86**, 3200 (2001).
- [5] M. E. Newman, *Physical review E* **66**, 016128 (2002).
- [6] R. Albert, H. Jeong, and A.-L. Barabási, *Nature* **406**, 378 (2000).
- [7] R. Cohen, K. Erez, D. Ben-Avraham, and S. Havlin, *Physical review letters* **85**, 4626 (2000).
- [8] D. S. Callaway, M. E. Newman, S. H. Strogatz, and D. J. Watts, *Physical review letters* **85**, 5468 (2000).
- [9] S. N. Dorogovtsev, A. V. Goltsev, and J. F. Mendes, *Reviews of Modern Physics* **80**, 1275 (2008).
- [10] S. V. Buldyrev, R. Parshani, G. Paul, H. E. Stanley, and S. Havlin, *Nature* **464**, 1025 (2010).
- [11] M. Szell, R. Lambiotte, and S. Thurner, *Proceedings of the National Academy of Sciences USA* **107**, 13636 (2010).
- [12] M. Barthélemy, *Physics Reports* **499**, 1 (2011).
- [13] M. De Domenico, A. Solé-Ribalta, S. Gómez, and A. Arenas, *Proceedings of the National Academy of Sciences USA* **111**, 8351 (2014).
- [14] J. Gao, S. V. Buldyrev, H. E. Stanley, and S. Havlin, *Nature physics* **8**, 40 (2012).
- [15] S.-W. Son, G. Bizhani, C. Christensen, P. Grassberger, and M. Paczuski, *EPL (Europhysics Letters)* **97**, 16006 (2012).
- [16] F. Radicchi, *Physical Review X* **4**, 021014 (2014).
- [17] S. D. Reis, Y. Hu, A. Babino, J. S. Andrade Jr, S. Canals, M. Sigman, and H. A. Makse, *Nature Physics* **10**, 762 (2014).
- [18] B. Bollobás, C. Borgs, J. Chayes, O. Riordan, et al., *The Annals of Probability* **38**, 150 (2010).
- [19] B. Karrer, M. E. J. Newman, and L. Zdeborová, *Physical Review Letters* **113**, 208702 (2014).
- [20] K. E. Hamilton and L. P. Pryadko, *Physical Review Letters* **113**, 208701 (2014).
- [21] K.-i. Hashimoto, *Automorphic forms and geometry of arithmetic varieties*. pp. 211–280 (1989).
- [22] F. Krzakala, C. Moore, E. Mossel, J. Neeman, A. Sly, L. Zdeborová, and P. Zhang, *Proceedings of the National Academy of Sciences* **110**, 20935 (2013).
- [23] F. Radicchi, *Physical Review E* **91**, 010801 (2015).
- [24] S. Hwang, S. Choi, D. Lee, and B. Kahng, arXiv preprint arXiv:1409.1147 (2014).
- [25] C. Stark, B.-J. Breitkreutz, T. Reguly, L. Boucher, A. Breitkreutz, and M. Tyers, *Nucleic acids research* **34**, D535 (2006).
- [26] M. De Domenico, M. A. Porter, and A. Arenas, *Journal of Complex Networks* p. cnu038 (2014).
- [27] *Bureau of transportation statistics*, <http://www.transtats.bts.gov>, accessed: 2015-01-18.
- [28] G. Bianconi and S. N. Dorogovtsev, arXiv preprint arXiv:1411.4160 (2014).
- [29] R. Guimerà, S. Mossa, A. Turtschi, and L. N. Amaral, *Proceedings of the National Academy of Sciences USA* **102**, 7794 (2005).
- [30] V. Colizza, A. Barrat, M. Barthélemy, and A. Vespignani, *Proceedings of the National Academy of Sciences USA* **103**, 2015 (2006).

γ	p_c	α	P_∞	β
2.3	0.18	0.34	0.01	0.33
2.7	0.25	0.43	0.07	0.39
3.5	0.33	0.60	0.16	0.54
100.0	0.47	0.95	0.32	1.09

Table S1: In panel f of Fig. 2, we fitted empirical estimations of the percolation threshold $p_c(N)$ computed at various system sizes N with the function $p_c(N) = p_c + N^{-\alpha}$. In Fig. 2g, we perform instead the fit $P_\infty(N) = P_\infty + N^{-\beta}$ for the height of the order parameter at criticality. Here, we report the values of the best estimates of p_c , α , P_∞ and β for the different values of the degree exponent γ used in the generation of the scale-free networks.

Appendix

Taylor expansions

An alternative way to arrive to the results of Eq. (3) is to use the multidimensional Taylor expansion of the r.h.s. of Eq. (1) around the trivial solution $\vec{s} = \vec{0}$ as

$$\begin{aligned} & [1 - \prod_{j \in \mathcal{N}_i} (1 - s_j)] \\ &= \sum_k s_k \frac{d}{ds_k} [1 - \prod_{j \in \mathcal{N}_i} (1 - s_j)] \Big|_{\vec{s}=\vec{0}} + o(s_i^2) . \\ &\simeq \sum_j A_{ij} s_j \end{aligned}$$

Truncated multidimensional Taylor expansions can be used also to reduce Eq. (5) to Eq. (8). The only difference here is that the derivatives are taken with respect to the variables $r_{i \rightarrow j}$, and the expansion is made around the trivial solution $\vec{r} = \vec{0}$.

When dealing with Eq. (9), the Taylor expansion should be instead extended to at least the second order. Let us first imagine that the intersection graph does not contain edges, so that Eq. (9) reads as

$$s_i = p S_{\mathcal{A}-\mathcal{B}_i} S_{\mathcal{B}-\mathcal{A}_i} .$$

Since $S_{\mathcal{A}-\mathcal{B}_i}$ and $S_{\mathcal{B}-\mathcal{A}_i}$ calculated at $\vec{s} = \vec{0}$ are zero, the first derivatives of the r.h.s. calculated in $\vec{s} = \vec{0}$ are automatically zero. The Taylor expansion of r.h.s. is thus

$$\begin{aligned} & \frac{1}{2} \sum_j \sum_k s_j s_k \frac{d^2}{ds_j ds_k} S_{\mathcal{A}-\mathcal{B}_i} S_{\mathcal{B}-\mathcal{A}_i} \Big|_{\vec{s}=\vec{0}} + o(s_i^3) = \\ & \frac{1}{2} \sum_j \sum_k s_j s_k \frac{d}{ds_j} S_{\mathcal{A}-\mathcal{B}_i} \frac{d}{ds_k} S_{\mathcal{B}-\mathcal{A}_i} \Big|_{\vec{s}=\vec{0}} + o(s_i^3) , \end{aligned}$$

where the second equality is justified by the fact that $S_{\mathcal{A}-\mathcal{B}_i}$ and $S_{\mathcal{B}-\mathcal{A}_i}$ are zero at $\vec{s} = \vec{0}$. Using the definitions of $S_{\mathcal{A}-\mathcal{B}_i}$ and $S_{\mathcal{B}-\mathcal{A}_i}$ we have that

$$\frac{d}{ds_j} S_{\mathcal{A}-\mathcal{B}_i} \Big|_{\vec{s}=\vec{0}} = A_{ij}(1 - B_{ij})$$

and

$$\frac{d}{ds_j} S_{\mathcal{B}-\mathcal{A}_i} \Big|_{\vec{s}=\vec{0}} = B_{ij}(1 - A_{ij}) ,$$

where A and B are the adjacency matrices of the network layers. In conclusion, we can approximate Eq. (9) in absence of the intersection term as

$$s_i = \frac{p}{2} \left[\sum_j s_j A_{ij}(1 - B_{ij}) \right] \left[\sum_j s_j B_{ij}(1 - A_{ij}) \right] .$$

With straightforward considerations, we can also insert the term accounting for the intersection graph, and write

$$s_i = p \sum_j A_{ij} B_{ij} s_j + \frac{p}{2} \left[\sum_j s_j A_{ij}(1 - B_{ij}) \right] \left[\sum_j s_j B_{ij}(1 - A_{ij}) \right] .$$

This last equation gives us some insights about the structure of the solution, but it does not allow to reduce the original problem to a simple eigenvalue/eigenvector equation as in the case of isolated networks. Similar considerations can be deduced by taking the Taylor expansion of Eq. (11).